A short splicing isoform of afadin suppresses the cortical axon branching in a dominant-negative manner

Kentaro Umeda[a], Nariaki Iwasawa[a], Manabu Negishi[a], and Izumi Oinuma[a,b]
[a]Laboratory of Molecular Neurobiology, Graduate School of Biostudies, Kyoto University, Sakyo-ku, Kyoto 606-8501, Japan; [b]PRESTO, Japan Science and Technology Agency, 4-1-8 Honcho Kawaguchi, Saitama 332-0012, Japan

ABSTRACT **Precise wiring patterns of axons are among the remarkable features of neuronal circuit formation, and establishment of the proper neuronal network requires control of outgrowth, branching, and guidance of axons. R-Ras is a Ras-family small GTPase that has essential roles in multiple phases of axonal development. We recently identified afadin, an F-actin–binding protein, as an effector of R-Ras mediating axon branching through F-actin reorganization. Afadin comprises two isoforms—l-afadin, having the F-actin–binding domain, and s-afadin, lacking the F-actin–binding domain. Compared with l-afadin, s-afadin, the short splicing variant of l-afadin, contains RA domains but lacks the F-actin–binding domain. Neurons express both isoforms; however, the function of s-afadin in brain remains unknown. Here we identify s-afadin as an endogenous inhibitor of cortical axon branching. In contrast to the abundant and constant expression of l-afadin throughout neuronal development, the expression of s-afadin is relatively low when cortical axons branch actively. Ectopic expression and knockdown of s-afadin suppress and promote branching, respectively. s-Afadin blocks the R-Ras–mediated membrane translocation of l-afadin and axon branching by inhibiting the binding of l-afadin to R-Ras. Thus s-afadin acts as a dominant-negative isoform in R-Ras-afadin–regulated axon branching.**

Monitoring Editor
Kozo Kaibuchi
Nagoya University

Received: Jan 22, 2015
Revised: Mar 13, 2015
Accepted: Mar 18, 2015

INTRODUCTION

Cortical neurons are highly polarized cells with a single long axon and multiple dendrites. They send out their axons to dendrites of distant target cells to carry information. The function of the nervous system depends on development of appropriate and complex connections of axons and dendrites. To achieve and maintain proper connections, multiple steps of axon development, such as axonal growth, guidance, and branching, must be strictly regulated by extrinsic cues and intrinsic signals (O'Donnell *et al.*, 2009; Bilimoria and Bonni, 2013). Of these steps, axon branching is fundamental to establish complex pattern of connectivity, and it is well established that formation of proper connections depends not only on guidance of their growth cones located at the axonal tips, but also on formation of branches from the shaft of the primary axon called collateral branches (Kalil *et al.*, 2000). Branches can be formed through two distinct modes: bifurcation of the growth cone at the tip of the axon and formation of branches, called collateral branches, from the axon shaft behind the advancing growth cone. Axon branching through axon bifurcation contributes to axon guidance, whereas formation of axon collateral branches is widely regarded as the major mechanism used to establish axon arbors in synaptic targets (Gallo, 2011). Formation of collateral branches is dependent on cytoskeletal regulation, and collateral branches are initiated by filamentous actin (F-actin)–based axonal protrusions, which subsequently become invaded by microtubules, thereby allowing the branch to mature and continue extending (Kalil *et al.*, 2000; Gallo, 2011).

This article was published online ahead of print in MBoC in Press (http://www.molbiolcell.org/cgi/doi/10.1091/mbc.E15-01-0039) on March 25, 2015.
The authors declare that they have no conflict of interest.
Address correspondence to: Izumi Oinuma (izu-oinuma@lif.kyoto-u.ac.jp).
Abbreviations used: ANOVA, analysis of variance; dbcAMP, dibutyryl cAMP; DIV, days in vitro; ERK, extracellular signal-regulated kinase; F-actin, filamentous actin; FBS, fetal bovine serum; GFP, green fluorescent protein; GST, glutathione *S*-transferase; HA, hemagglutinin; HRP, horseradish peroxidase; PBS, phosphate-buffered saline; PDZ, PSD-95/Dlg/ZO-1; PI3K, phosphatidylinositol 3-kinase; PMSF, phenylmethylsulfonyl fluoride; RA, Ras association; shRNA, short hairpin RNA; RBD, Ras-binding domain; TBS, Tris-buffered saline; YFP, yellow fluorescent protein.

Extensive studies revealed that Ras and Rho-family small GTPases are involved in control of neuronal morphology by regulation of the actin and microtubule cytoskeleton (Hall and Lalli, 2010; Spillane and Gallo, 2014). Small GTPases serve as molecular switches by cycling between the GDP-bound inactive state and a GTP-bound active state, and GTP-bound active small GTPases interact with their specific effectors to induce various biological events on cells. Among the Ras-family proteins, R-Ras–subfamily proteins, R-Ras, TC21 (R-Ras2), and M-Ras (R-Ras3), show relatively similar homology and form a distinct branch from the classical Ras subfamily comprising H-Ras, K-Ras, and N-Ras (Matsumoto *et al.*, 1997). The classical Ras proteins primarily mediate cell growth and differentiation through the kinase-mediated pathways of extracellular signal-regulated kinase (ERK) and phosphatidylinositol 3-kinase (PI3K), whereas R-Ras functions as a regulator of cell morphology in a variety of cells, including neurons (Kinbara *et al.*, 2003; Arimura and Kaibuchi, 2007; Oinuma *et al.*, 2007). R-Ras contributes to activation of PI3K but not ERK, and R-Ras is also an activator of a cell–substrate adhesion molecule, integrin (Zhang *et al.*, 1996; Keely *et al.*, 1999; Komatsu and Ruoslahti, 2005). We previously reported that R-Ras plays essential roles in axon formation, elongation, and guidance (Oinuma *et al.*, 2004a,b, 2007). During cortical axon development, cultured neurons first extend several undifferentiated neurites (at stages 1 and 2), and then, at stages 2 and 3, one of the neurites begins to elongate rapidly to become the axon, and subsequent axonal branching occurs (Bradke and Dotti, 2000). R-Ras selectively accumulates in the future axon of stage 2 neurons, and its activity increases after plating and peaks between stages 2 and 3, when neuronal polarization and axon formation occur (Oinuma *et al.*, 2007). R-Ras functions as a regulator for both actin and microtubule cytoskeletons in neurons during axon development. We showed that R-Ras contributes to microtubule-dependent regulation of axonal morphology through a series of PI3K signaling, inducing activation of a microtubule-assembly promoter, collapsin response mediator protein-2 (Ito, Oinuma, *et al.*, 2006; Oinuma *et al.*, 2007). Furthermore, we showed that afadin, an F-actin–binding protein, functions as an effector for R-Ras–mediated cortical and hippocampal axon branching (Iwasawa *et al.*, 2012).

Afadin, whose human orthologue is called AF-6, was originally purified from the cytosol fraction of rat embryonic brain and is a multidomain adaptor protein having two Ras association (RA) domains, a PSD-95/Dlg/ZO-1 (PDZ) domain, and the carboxyl-terminal F-actin–binding domain (Mandai *et al.*, 1997; Takai *et al.*, 2008). The afadin PDZ domain is responsible for binding to nectins, the immunoglobulin superfamily cell adhesion molecules localized in epithelial cells (Takahashi *et al.*, 1999; Kurita *et al.*, 2011). In addition to nectins, afadin interacts with various proteins involved in maintenance of adherence junctions and contributes to cell–cell adhesion (Tachibana *et al.*, 2000; Pokutta *et al.*, 2002; Asada *et al.*, 2003). In addition to the control of cell–cell adhesion, afadin regulates cell migration of normal fibroblasts and cancer cells (Miyata *et al.*, 2009; Fournier *et al.*, 2011). In neurons, several reports have shown that afadin controls dendritic spine morphology, and neuron-specific afadin conditional knockout mice exhibited decrease in spine and excitatory synapse densities (Xie *et al.*, 2005; Beaudoin *et al.*, 2012). Afadin localizes not only in dendrites, but also in axons (Lim *et al.*, 2008), and we showed that active R-Ras interacts with the RA domains of afadin to induce translocation of afadin to the membranes, promoting cortical axon branching (Iwasawa *et al.*, 2012).

Afadin comprise two isoforms, l-afadin (205 kDa) and s-afadin (190 kDa; Mandai *et al.*, 1997). We showed that l-afadin with active R-Ras promotes axon branching through F-actin reorganization mediated by the F-actin–binding domain of l-afadin (Iwasawa *et al.*, 2012). Compared with l-afadin, s-afadin, the short splicing variant of l-afadin, contains RA domains but lacks the carboxyl-terminal F-actin–binding domain (Mandai *et al.*, 1997). The two afadin isoforms display distinct tissue expression patterns; l-afadin is ubiquitously expressed, whereas s-afadin is brain specific (Mandai *et al.*, 1997). It was recently shown that s-afadin is expressed in neurons but not in astroglial cells (Kobayashi *et al.*, 2014), suggesting a role of s-afadin in neuronal functions. However, the roles of s-afadin in neurons remain poorly understood. In this study, we show that s-afadin acts as a dominant-negative suppressor for R-Ras–mediated cortical axon branching.

RESULTS

Expression of s-afadin is relatively low when cortical axons branch actively

Afadin comprises two isoforms, l-afadin (205 kDa) and s-afadin (190 kDa; Mandai *et al.*, 1997). We reported that l-afadin, an F-actin–binding protein containing RA domains, is an effector of R-Ras, promoting axon branching through F-actin reorganization (Iwasawa *et al.*, 2012). Because s-afadin, the short splicing variant of l-afadin, contains RA domains but lacks the carboxyl-terminal F-actin–binding domain (Mandai *et al.*, 1997; Figure 1A) we first examined whether s-afadin associates with R-Ras. Immunoprecipitation analysis showed that both isoforms bound to R-Ras QL, a constitutively active form of R-Ras (Figure 1B). We next examined the endogenous expression of the afadin isoforms in primary cultured rat cortical neurons during the stages of axon development. In our culture conditions, cortical axons actively branch during 0–3 d in vitro (DIV), and then axons elongate during the later period of 3–6 DIV (Iwasawa *et al.*, 2012). As shown in Figure 1C, abundant and constant expression of l-afadin throughout the stages of axonal development was observed. In contrast, expression of s-afadin was relatively low during 0–3 DIV, the period of branch formation, and gradually increased in the later period of 3–9 DIV, suggesting the opposite correlation of the expression pattern of s-afadin with cortical axon branch formation. We also examined expression of afadin isoforms in the developing rat brain. Immunoblot analysis of rat whole-brain lysates from embryonic day 16 (E16) to postnatal day 14 (P14) showed that expression of endogenous s-afadin in the brain was low during embryonic stages and increased after birth (Figure 1D).

Ectopic expression of s-afadin suppresses cortical axon branching

To study the role of s-afadin in axonal branch formation, we performed overexpression analysis of s-afadin. Cortical neurons were transfected with yellow fluorescent protein (YFP) and either Myc-tagged l-afadin or s-afadin at 1 DIV, and their axonal morphology was observed at 3 DIV (Figure 2). As we reported, ectopic expression of l-afadin promoted axon branching, but not elongation, compared with expression of YFP alone, showing a specific role for l-afadin in axon branching (Iwasawa *et al.*, 2012). In contrast, the overexpression of s-afadin suppressed basal axon branching without affecting axon length. These results represent the opposite regulation of cortical axon branching by two afadin isoforms, l-afadin and s-afadin; the former potentiates and the latter blocks branching activity of cortical axons, and lowered expression of s-afadin is required for active axon branching.

RA domains are responsible for s-afadin–mediated suppression of cortical axon branching

Branch-promoting activity of l-afadin requires R-Ras binding to RA domains (Iwasawa *et al.*, 2012), and s-afadin also contains RA

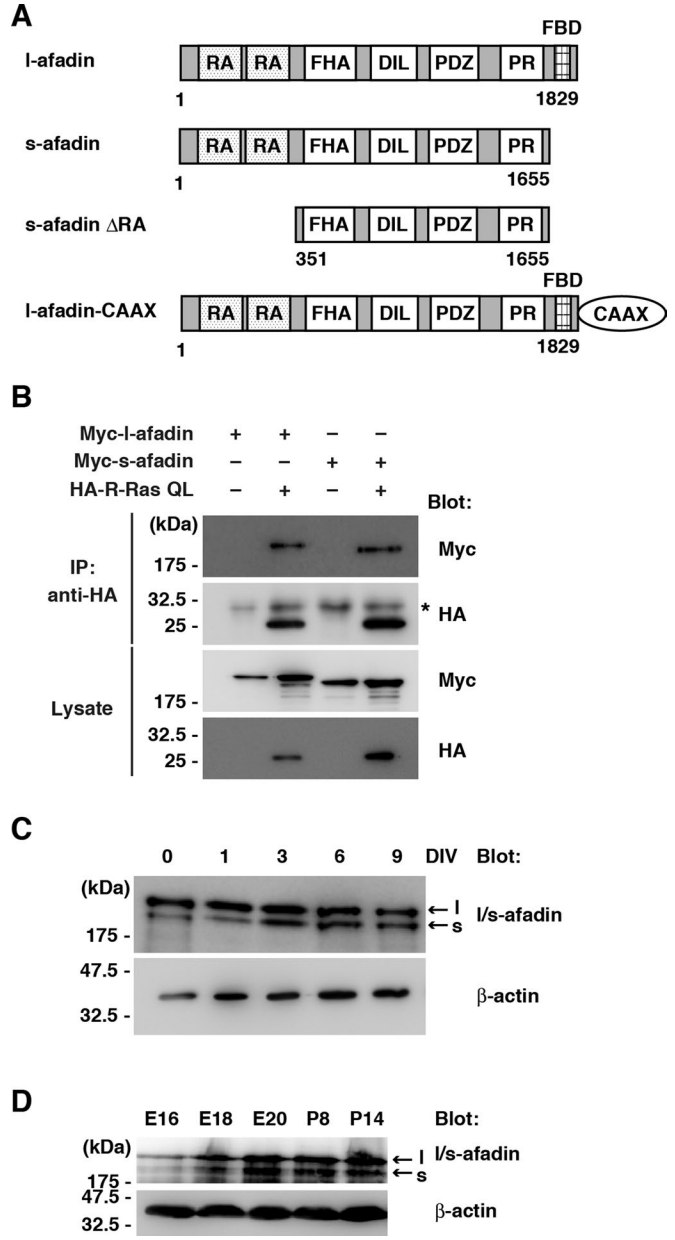

FIGURE 1: Expression patterns of two afadin isoforms during cortical neuronal development and their ability to bind to active R-Ras. (A) Schematic structures of afadin constructs used in this study. CAAX, CAAX sequences, where C represents cysteine, A is an aliphatic amino acid, and X is a terminal amino acid; DIL, dilute domain; FBD, F-actin–binding domain; FHA, forkhead-associated domain; PR, proline-rich region; RA, Ras association domain. Numbers indicate amino acid positions within the sequence. (B) Lysates from HEK293T cells transfected with Myc-tagged afadin and HA-tagged R-Ras QL (constitutively active mutant) were immunoprecipitated with anti-HA antibody. Lysate inputs and immunoprecipitates were analyzed by immunoblotting. Asterisk indicates the position of the immunoglobulin light chains. (C, D) Developmental expression of afadin in cultured cortical neurons (C) or whole-brain lysates (D) at the indicated time points was analyzed by immunoblotting with anti–l/s-afadin antibody. Both the long (l) and short (s) afadin isoforms were detected.

domains and has ability to bind to active R-Ras (Figure 1B). To determine the roles of RA domains in s-afadin–mediated suppression of axon branching activity, we generated s-afadin ΔRA, which lacks RA domains (Figure 1A). Cortical neurons were transfected with YFP and either Myc-tagged s-afadin or s-afadin ΔRA at 1 DIV and their axonal morphology was observed at 3 DIV (Figure 3). Overexpression of s-afadin blocked basal axon branching, whereas that of s-afadin ΔRA had no effect on axon branching. These results suggest that RA domains are responsible for s-afadin–mediated suppression of basal branching activity of cortical neurons. We further examined the effect of s-afadin on active R-Ras–induced cortical axon branching. As shown in Figure 4, ectopic expression of s-afadin but not that of s-afadin ΔRA blocked active R-Ras–induced cortical axon branching. These results suggest that s-afadin blocks R-Ras–mediated axon branching in an RA domain–dependent manner.

s-Afadin blocks membrane translocation of l-afadin induced by active R-Ras

Regulation of membrane localization of l-afadin is important for its various cellular functions, such as directional cell migration of fibroblast cells and dendritic spine morphogenesis of neurons (Xie *et al.*, 2005; Miyata *et al.*, 2009), and we reported that active R-Ras induces the membrane translocation of l-afadin via its binding to R-Ras through RA domains (Iwasawa *et al.*, 2012). As shown in Figure 5, A and B, active R-Ras also induced the membrane translocation of s-afadin, as well as that of l-afadin. Thus active R-Ras can translocate both of the afadin isoforms to the membrane. We therefore examined whether coexistence of s-afadin with l-afadin affects the R-Ras–induced membrane translocation of l-afadin. Neuro2a cells transfected with hemagglutinin (HA)-tagged R-Ras QL and green fluorescent protein (GFP)–tagged l-afadin with or without Myc-tagged s-afadin were subjected to subcellular fractionation analysis. As shown in Figure 5C, coexpression of s-afadin severely impaired the R-Ras–induced membrane translocation of l-afadin. We further tested whether l-afadin and s-afadin are competitive with each other in R-Ras QL–induced membrane localization. To test this, we coexpressed a constant amount of l-afadin and increasing amounts of s-afadin with R-Ras QL in Neuro2a cells. As shown in Figure 5D, when expression of s-afadin exceeds that of l-afadin, membrane localization of l-afadin was strongly suppressed. Intriguingly, most of the overexpressed s-afadin was localized in the cytosolic fraction. These results suggest that l-afadin and s-afadin are competitive with each other for R-Ras QL–induced membrane localization.

s-Afadin blocks binding of l-afadin to active R-Ras in a dominant-negative manner

Next we sought to identify the molecular mechanisms by which s-afadin blocks R-Ras QL–induced membrane translocation of l-afadin. Because active R-Ras binding to the RA domains triggers membrane translocation of l-afadin (Iwasawa *et al.*, 2012), we tested whether s-afadin inhibits R-Ras binding to l-afadin. We expressed HA-tagged R-Ras QL and Myc-tagged afadin isoforms in Neuro2a cells and immunoprecipitated the lysates with anti-HA antibody. When l-afadin and s-afadin were coexpressed, the binding of both isoforms to R-Ras was decreased, suggesting that l-afadin and s-afadin are competitive with each other for R-Ras binding (Figure 6A, rightmost lane). It has been reported that AF-6 type-1, a human orthologue of afadin, self-associates through the RA domains (Liedtke *et al.*, 2010). The immunoprecipitation analysis revealed that l-afadin precipitated more s-afadin than l-afadin itself (Figure 6B). We next examined the effect of s-afadin on the binding of l-afadin to active R-Ras. s-Afadin suppressed the binding of l-afadin to active R-Ras. On the other hand, the interaction of s-afadin and l-afadin was disturbed by the presence of active R-Ras (Figure 6C). These results show mutually exclusive binding of s-afadin and R-Ras to

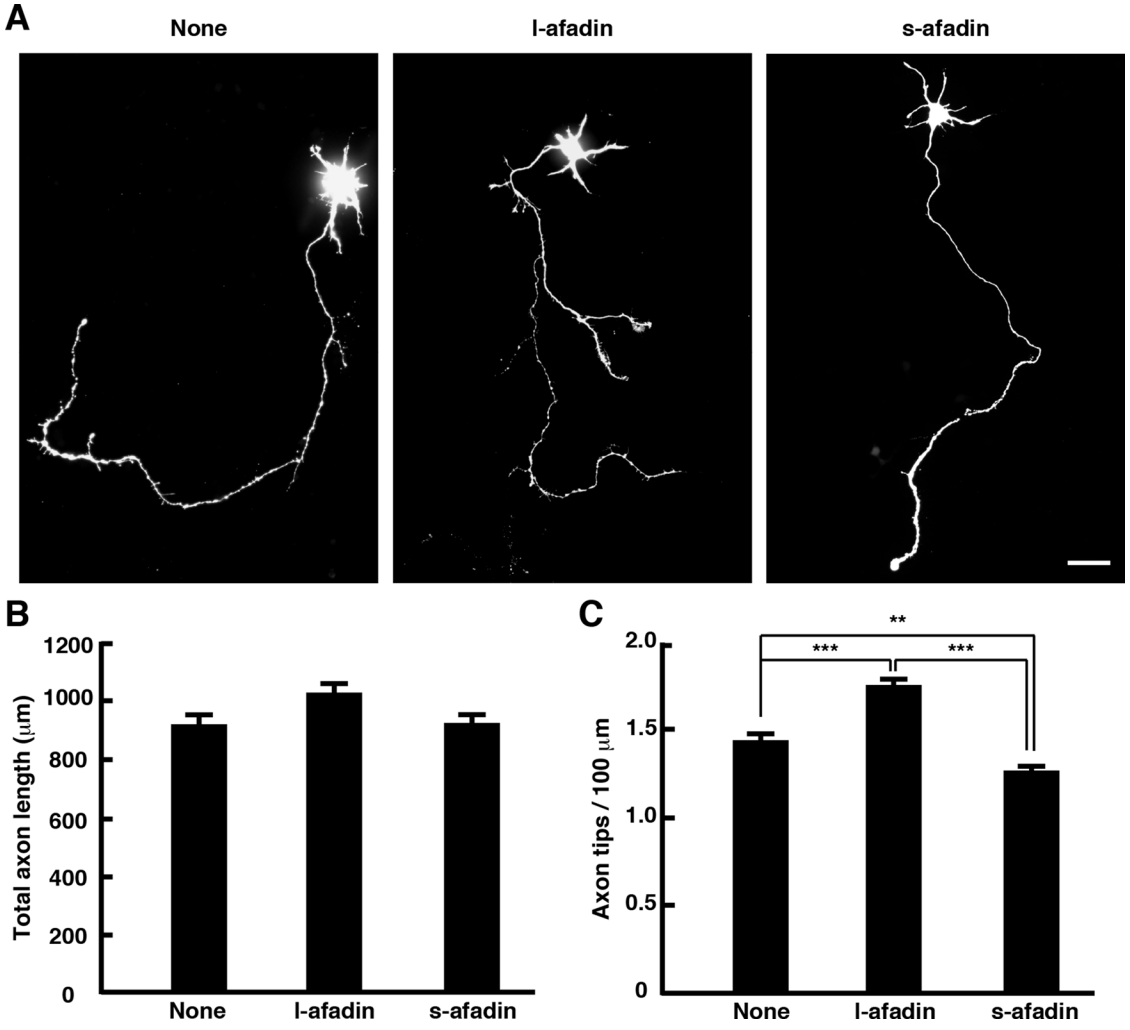

FIGURE 2: Ectopic expression of l-afadin promotes axon branching, whereas that of s-afadin suppresses axon branching. (A) Primary cultured rat cortical neurons were transfected with YFP and l- or s-afadin plasmid at 1 DIV and fixed at 3 DIV. The fluorescence images of YFP are shown. Scale bar, 50 μm. (B, C) Total axon length (B) and axon tip number/100 μm (C) were measured. The results are means ± SEM of three independent experiments ($n = 45$; $^{**}p < 0.01$; $^{***}p < 0.001$, one-way ANOVA with Dunnett's post hoc test).

l-afadin, indicating that s-afadin blocks the binding of l-afadin to active R-Ras in a dominant-negative manner.

Forced membrane targeting of l-afadin overcomes the inhibitory effect of s-afadin on axon branching

We identified that s-afadin blocks membrane translocation of l-afadin in a dominant-negative manner (Figures 5 and 6), and we therefore examined whether decreased membrane localization of l-afadin is responsible for s-afadin–induced reduction of cortical axon branching. We fused the CAAX sequence of K-Ras to the carboxyl-terminal of l-afadin (l-afadin-CAAX; Figure 1A) to generate a membrane targeting form of l-afadin. R-Ras–independent artificial membrane targeting of l-afadin-CAAX was verified by subcellular fractionation analysis of transiently transfected Neuro2a cells, and this localization was not blocked by overexpression of s-afadin in Neuro2a cells (Figure 7A). The l-afadin–induced promotion of cortical axon branching was blocked by coexpression of s-afadin. Cortical neurons transfected with l-afadin-CAAX displayed more highly branched axons than l-afadin–transfected cells, and expression of s-afadin did not block the promotion of axon branching induced by l-afadin-CAAX, showing that forced membrane targeting of l-afadin overcame the inhibitory effect of s-afadin on axon branching (Figure 7, B and C). These data suggest that decreased membrane localization of l-afadin is responsible for s-afadin–mediated inhibition of cortical axon branching.

Knockdown of endogenous s-afadin promotes membrane translocation of l-afadin and axon branching

To study the roles of endogenous s-afadin in membrane localization of l-afadin and cortical axon branching, we generated short hairpin RNA (shRNA) expression vectors designed to specifically target each isoform of afadin. Each shRNA effectively and specifically silenced the endogenous expression of each afadin isoform and did not inhibit the expression of other (Figure 8A). Subcellular fractionation analysis revealed that depletion of endogenous s-afadin by s-afadin–specific shRNA increased the membrane localization of l-afadin in 4-DIV cortical neurons (Figure 8B). We further examined the effect of each of the afadin isoform–specific shRNAs on axonal morphology. Cortical neurons were transfected with YFP and shRNAs before plating, and their axonal morphology was analyzed at 4 DIV.

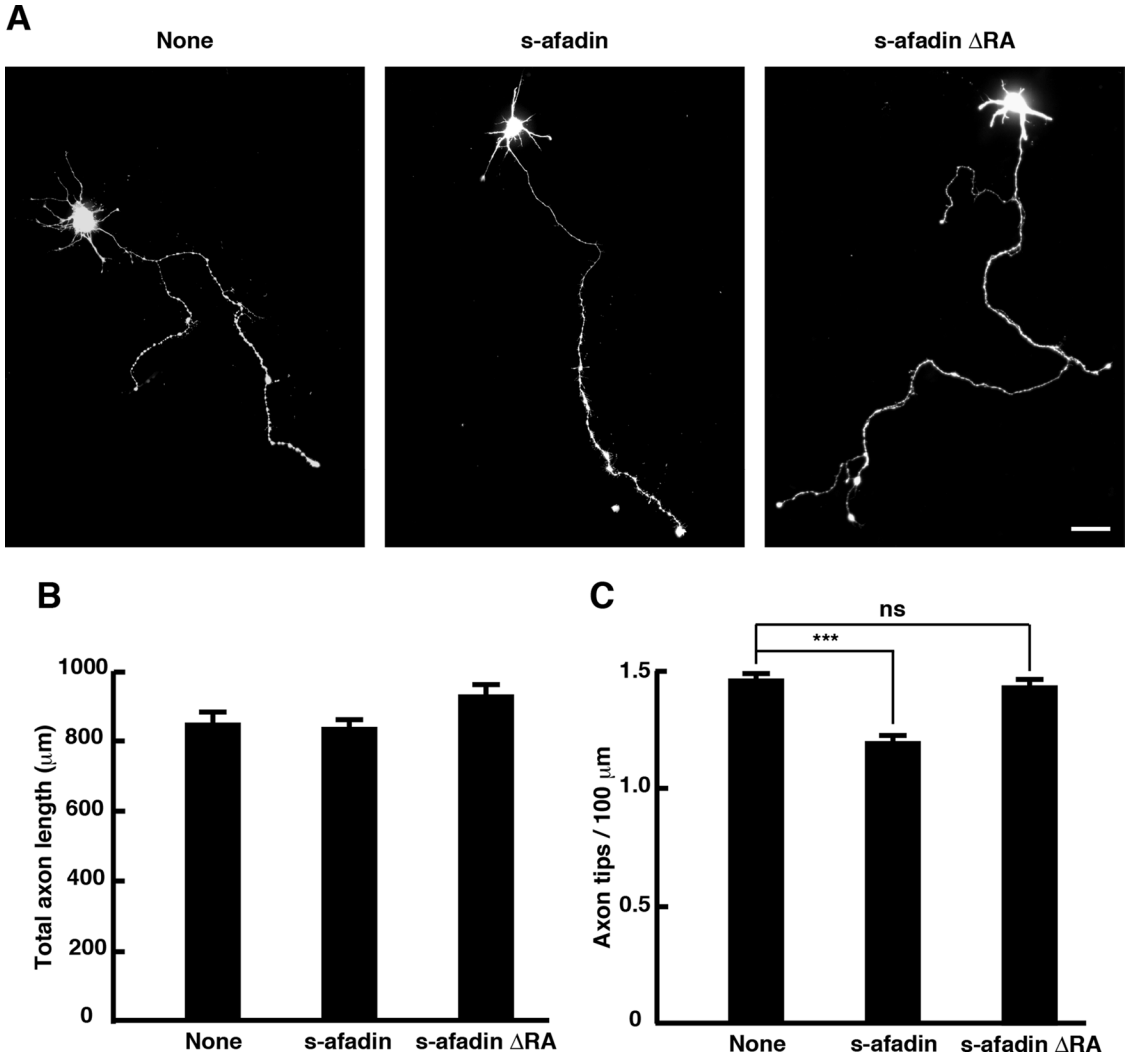

FIGURE 3: The RA domains are responsible for s-afadin–mediated suppression of cortical axon branching. (A) Primary cultured rat cortical neurons were transfected with YFP and s-afadin or s-afadin ΔRA plasmid at 1 DIV and fixed at 3 DIV. The fluorescence images of YFP are shown. Scale bar, 50 μm. (B, C) Total axon length (B) and axon tip number/100 μm (C) were measured. The results are means ± SEM of three independent experiments ($n = 45$; ns, not significant; ***$p < 0.001$, one-way ANOVA with Dunnett's post hoc test).

Expression of the l-afadin–specific shRNA suppressed cortical axon branching, whereas that of the s-afadin–specific shRNA enhanced branching (Figure 8, C–E). These data together suggest that endogenous s-afadin blocks basal branching activity of cortical neurons by inhibiting membrane localization of l-afadin.

Dibutiryl cAMP induces R-Ras activation and membrane localization of l-afadin

Cyclic nucleotides are well known as key players in axon guidance (Tojima *et al.*, 2011), and cAMP has been reported to trigger axon branching (Mingorance-Le Meur and O'Connor, 2009; Gallo, 2011). We asked whether cAMP could affect endogenous R-Ras activity in cortical neurons. The treatment of 3-DIV cortical neurons with a membrane-permeable cAMP analogue, dibutiryl cAMP (dbcAMP), induced a significant increase of endogenous R-Ras activity (Figure 9, A and B), and immunoprecipitation assay showed that dbcAMP treatment enhanced the interaction between l-afadin and R-Ras in cortical neurons (Figure 9C). cAMP also increased membrane localization of l-afadin, and knockdown of endogenous R-Ras by R-Ras–specific shRNA (Oinuma *et al.*, 2007) suppressed the membrane localization (Figure 9D). These results suggest that elevation of intracellular cAMP functions as a trigger for cortical axon branching, inducing R-Ras activation and R-Ras–mediated membrane localization of l-afadin.

DISCUSSION

Collateral branches of cortical axons are considered to be generated de novo from the main axon, and negative regulation of axon branching is crucial for the formation of the proper neuronal network (Mingorance-Le Meur and O'Connor, 2009; Gallo, 2011). In contrast to the well-studied molecules involved in promotion of axon branching, molecular mechanisms that block axon branching have remained poorly understood. We report here a novel mechanism by which s-afadin, a short splicing isoform of l-afadin, acts as a suppressor of cortical axon branching.

Axon branching is preceded by a reorganization of the cytoskeleton in the axon shaft (Kalil *et al.*, 2000; Dent and Kalil, 2001). The cytoskeletal remodeling includes fragmentation of microtubules

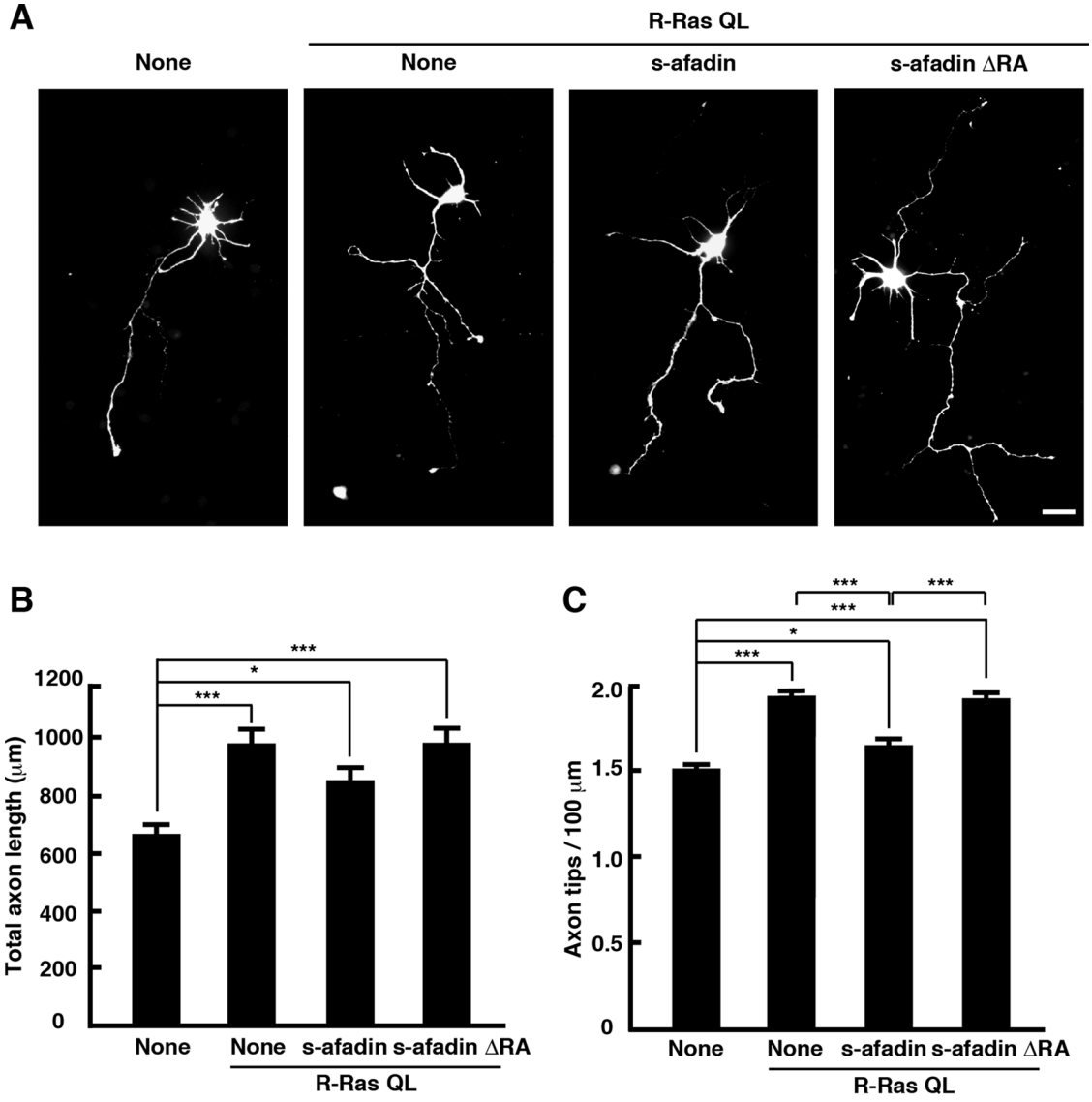

FIGURE 4: Ectopic expression of s-afadin blocks R-Ras–mediated axon branching in an RA domain–dependent manner. (A) Cortical neurons were transfected with YFP, R-Ras QL, and the indicated afadin plasmids at 0 DIV before plating using nucleofection technology and fixed at 3 DIV. The fluorescence images of YFP are shown. Scale bar, 50 μm. (B, C) Total axon length (B) and axon tip number/100 μm (C) were measured. The results are means ± SEM of three independent experiments ($n = 45$; *$p < 0.05$; ***$p < 0.001$, one-way ANOVA with Dunnett's post hoc test).

and subsequent local accumulation of F-actin, called actin patches, along the axon shaft, where the formation of actin-driven protrusions, such as filopodia and lamellipodia, and subsequent branch generation occur (Loudon *et al.*, 2006). We recently reported that l-afadin, an F-actin–linked multidomain adaptor protein, functions as an effector for R-Ras, inducing cortical axon branching through remodeling of F-actin (Iwasawa *et al.*, 2012). The RA domains of l-afadin are the binding sites for R-Ras, and R-Ras binding triggers membrane targeting of l-afadin, inducing axon branching. On the other hand, the carboxyl-terminal F-actin–binding domain within l-afadin is a functional domain responsible for axon branching. Compared with l-afadin, s-afadin, the short splicing variant of l-afadin, contains RA domains but lacks the carboxyl-terminal F-actin–binding domain (Mandai *et al.*, 1997). We first presumed a simple competition model in which s-afadin competes with l-afadin for R-Ras binding, causing suppression of membrane localization of l-afadin concomitant with decreased R-Ras bound to l-afadin. However, a series of studies showed that s-afadin inhibits cortical axon branching in an efficient way. We found that s-afadin binds to l-afadin, and this binding obstructs the binding of R-Ras to l-afadin, inhibiting cortical axon branching in a dominant-negative manner. To our knowledge, this is the first example of negative regulation of cortical axon branching through alternative splicing by which a short alternative splice form exerts a dominant-negative effect on the other isoform that triggers axon branching.

Tissue- and cell type–specific alternative splicing profoundly contributes to many aspects of animal development, and this is nowhere more evident than in the nervous system, especially in production of synaptic diversity at the later stages of neuronal development (Grabowski and Black, 2001; Schreiner *et al.*, 2014). Northern and Western blot analyses showed that the two afadin isoforms display distinct tissue expression patterns; l-afadin is ubiquitously expressed, whereas s-afadin is brain specific (Mandai *et al.*, 1997). It was recently shown that s-afadin is expressed in neurons but not in

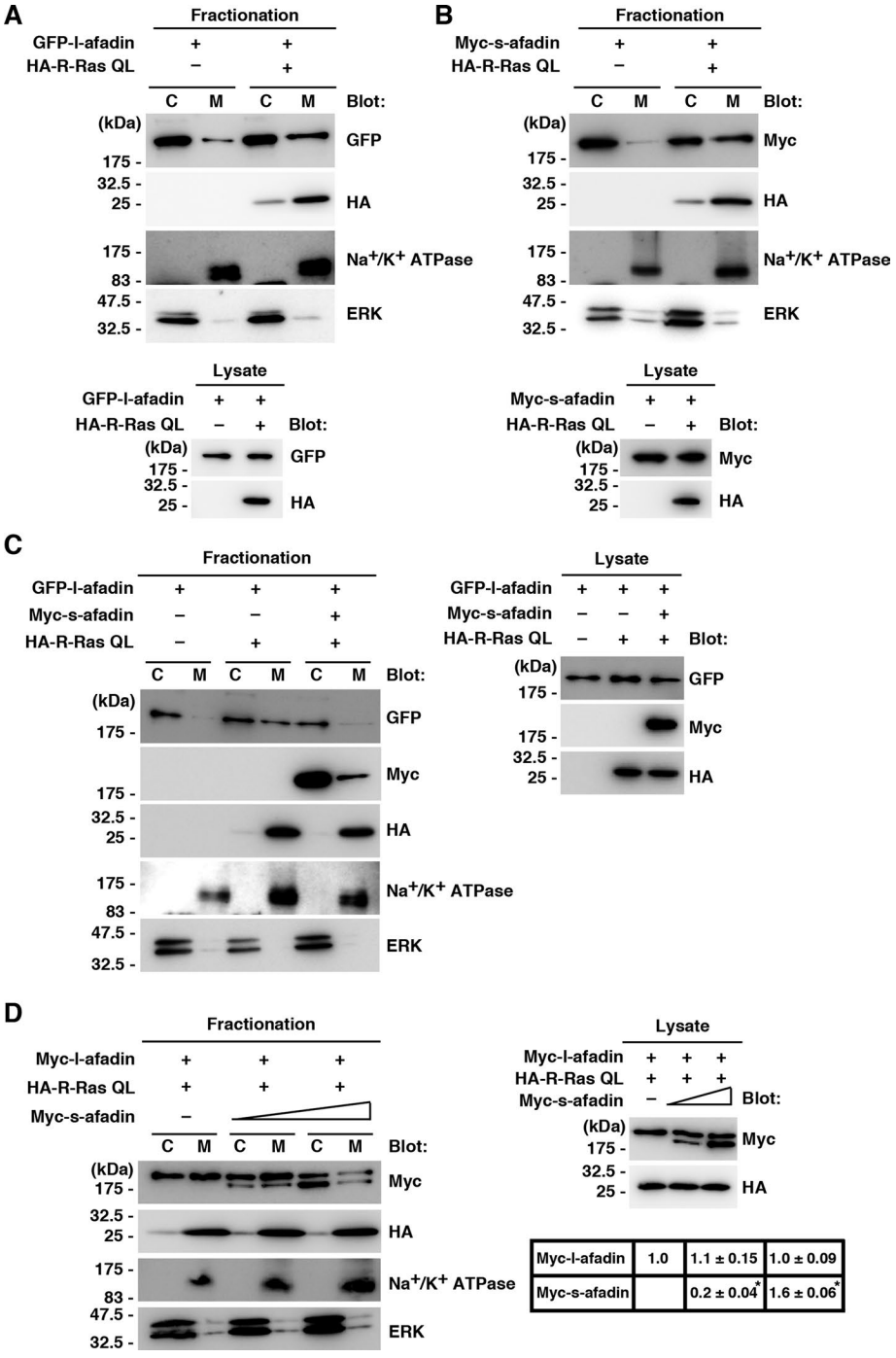

Myc-l-afadin	1.0	1.1 ± 0.15	1.0 ± 0.09
Myc-s-afadin		0.2 ± 0.04*	1.6 ± 0.06*

FIGURE 5: s-Afadin blocks membrane translocation of l-afadin induced by active R-Ras. (A–D) Cellular homogenates from Neuro2a cells transfected with the indicated expression plasmids were separated into cytosolic (C) and membrane (M) fractions. A constant amount of l-afadin and R-Ras QL and increasing amounts of s-afadin were coexpressed in cells (D). The table shows the quantification and statistical comparison of the expression level of the afadin isoforms in total cell lysate by densitometry of the Western blot bands. The value of Myc-l-afadin alone was defined as 1, and relative expression of individual afadin was assessed ($n = 3$; means ± SEM; *$p < 0.05$, one-way ANOVA with Dunnett's post hoc test). (D) The fractionated samples and total lysates were analyzed by immunoblotting with anti-Myc or anti-HA antibody. These fractions were also immunoblotted with anti–Na^+/K^+ ATPase α subunit antibody for the control membrane protein and with anti-ERK antibody for the control cytosolic protein. The immunoblot results shown are representative of three (A, B, D) or four (C) independent experiments that yielded similar results. Quantitative densitometry and statistical analysis of the Western blot bands are included in Supplemental Figure S1.

astroglial cells (Kobayashi *et al.*, 2014). We showed here that expression of s-afadin in cultured cortical neurons is relatively low at the earlier stage of neuronal development, when axons branch actively, and the lower level of s-afadin expression rather than that of l-afadin is required for axon branching. Knockdown of endogenous s-afadin augments basal axon branching, suggesting that the expression level of s-afadin critically regulates axon branch formation. Further studies are required to identify the splicing factors and/or regulators of mRNA stability, as well as their upstream regulators, that contribute to the expression control of s-afadin in cortical axons.

Many extracellular cues and neuronal activity are implicated in regulation of axonal morphology (Dent and Kalil, 2001; Yamada *et al.*, 2010; Bilimoria and Bonni, 2013). It has been reported that an attractive axon guidance factor netrin-1 promotes axon branching, whereas repulsive guidance factors such as semaphorins and ephrins suppress it (Dent *et al.*, 2004, Bilimoria and Bonni, 2013). Netrin is known to increase intracellular cAMP in neurons, and elevation of cAMP is required for netrin-mediated axonal attraction and elongation (Höpker *et al.*, 1999; Corset *et al.*, 2000). Emerging evidence suggests that signal transductions of multiple attractive and repulsive factors are integrated into the intracellular cAMP level (Tojima *et al.*, 2011). Elevation of cAMP is considered to function as a trigger for cortical axon branching by inducing deconsolidation of axon shaft (Mingorance-Le Meur and O'Connor, 2009; Gallo, 2011). In our study using whole-cell lysate of dbcAMP-treated cortical neurons, we observed a significant increase in endogenous R-Ras activity and R-Ras–mediated membrane targeting of l-afadin. It is interesting to note that the cAMP-induced membrane localization is also observed with s-afadin. This suggests that s-afadin dominant negatively blocks the membrane localization of l-afadin, but once localized to the membrane when abundant active R-Ras is available to afadins, s-afadin no longer functions as a dominant negative for l-afadin. Our previous immunofluorescence analysis of 2-DIV cortical neurons, where expression level of s-afadin is very low, using anti–l/s-afadin antibody shows that afadin accumulates at the site of budding protrusions located at the axonal tips and shafts, where it is well colocalized with F-actin (Iwasawa *et al.*, 2012). Unfortunately, s-afadin–specific antibody has not been available. Therefore we have no way to check whether endogenous

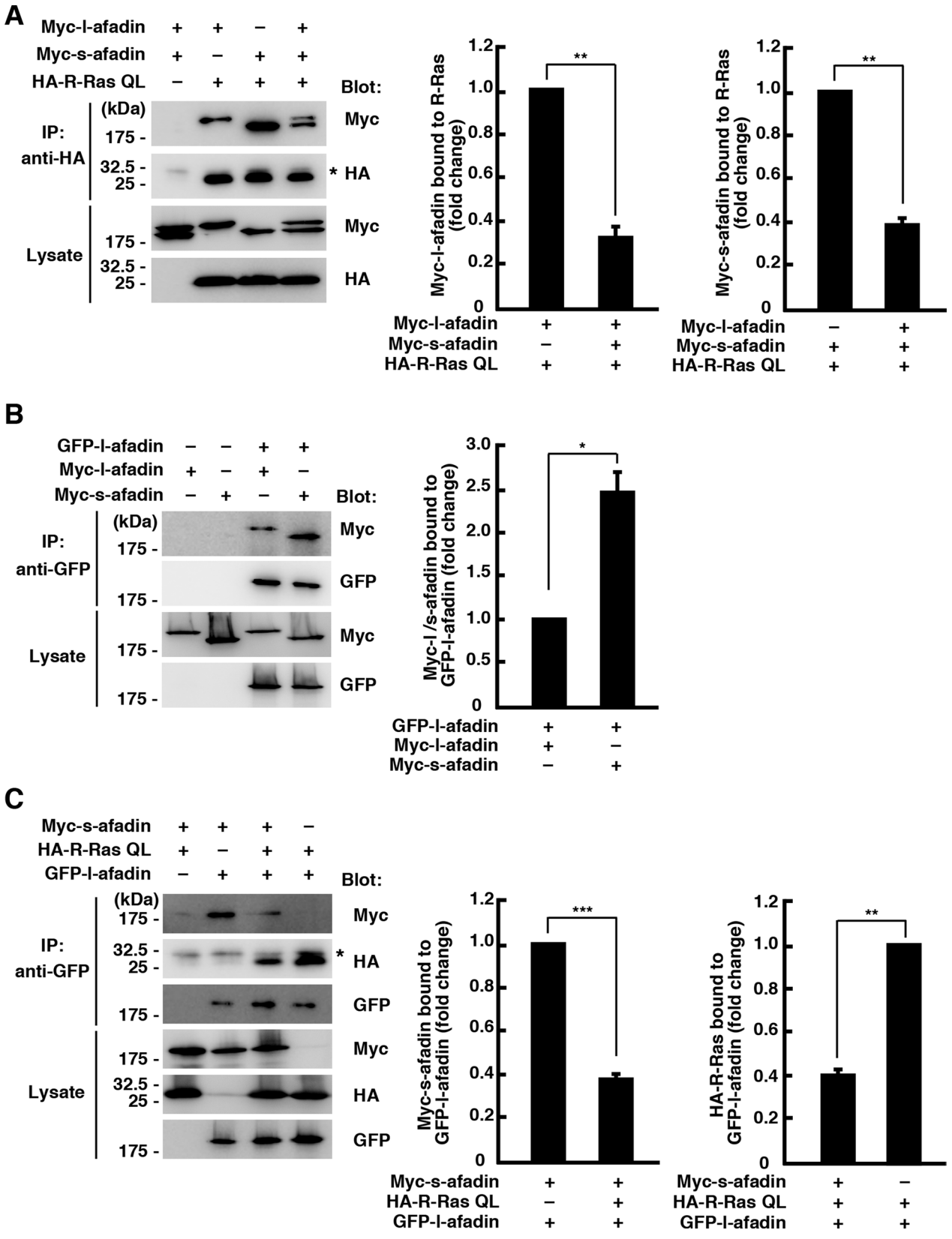

FIGURE 6: s-Afadin blocks binding of l-afadin to active R-Ras in a dominant-negative manner. (A–C) Cells lysates from Neuro2a cells expressing the indicated plasmids were immunoprecipitated with anti-HA antibody (A) or anti-GFP antibody (B, C). Lysate inputs and immunoprecipitates were analyzed by immunoblotting. Asterisk indicates the position of the immunoglobulin light chains. The immunoblots shown are representative of three (A, B) or four (C) independent experiments that yielded similar results. The graphs show quantitative densitometry and statistical analysis of the Western blot bands (means ± SEM; *$p < 0.05$; **$p < 0.01$; ***$p < 0.001$, Student's *t* test).

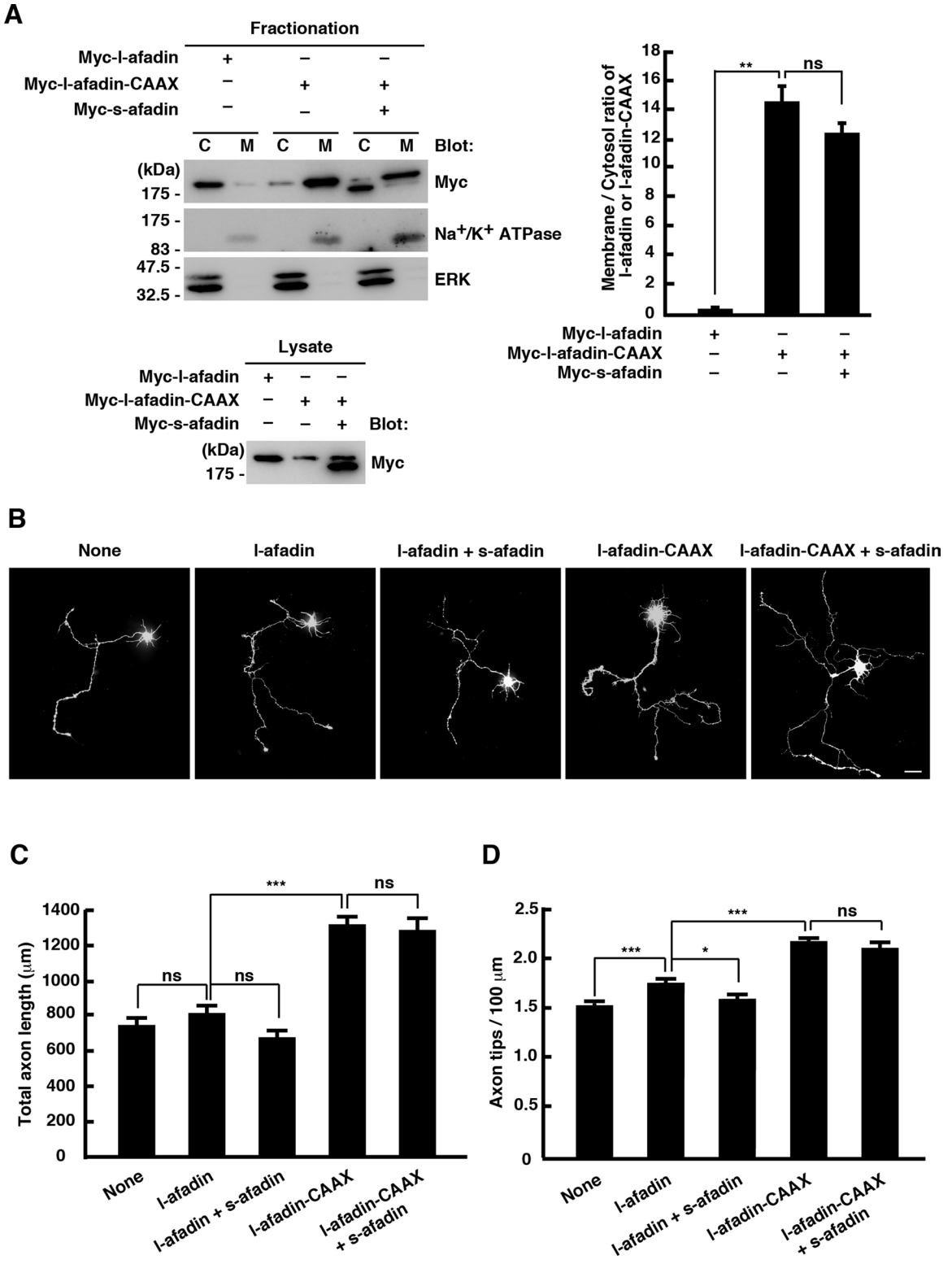

FIGURE 7: Forced membrane targeting of l-afadin overcomes the inhibitory effect of s-afadin on axon branching. (A) Cellular homogenates from Neuro2a cells expressing Myc-tagged l-afadin, l-afadin-CAAX, or s-afadin were separated into cytosolic (C) and membrane (M) fractions. The fractionated samples and total lysates were analyzed by immunoblotting. The immunoblots shown are representative of four independent experiments that yielded similar results. The graph shows quantitative densitometry and statistical analysis of the Western blot bands ($n = 4$; means ± SEM; ns, not significant; $^{**}p < 0.01$, one-way ANOVA with Dunnett's post hoc test). (B) Primary cultured rat cortical neurons were transfected with the indicated plasmid at 1 DIV and fixed at 3 DIV. The fluorescence images of YFP are shown. Scale bar, 50 μm. (C, D) Total axon length (C) and axon tip number/100 μm (D) were measured. The results are means ± SEM of three independent experiments ($n = 45$; ns, not significant; $^{*}p < 0.05$; $^{**}p < 0.01$; $^{***}p < 0.001$, one-way ANOVA with Dunnett's post hoc test).

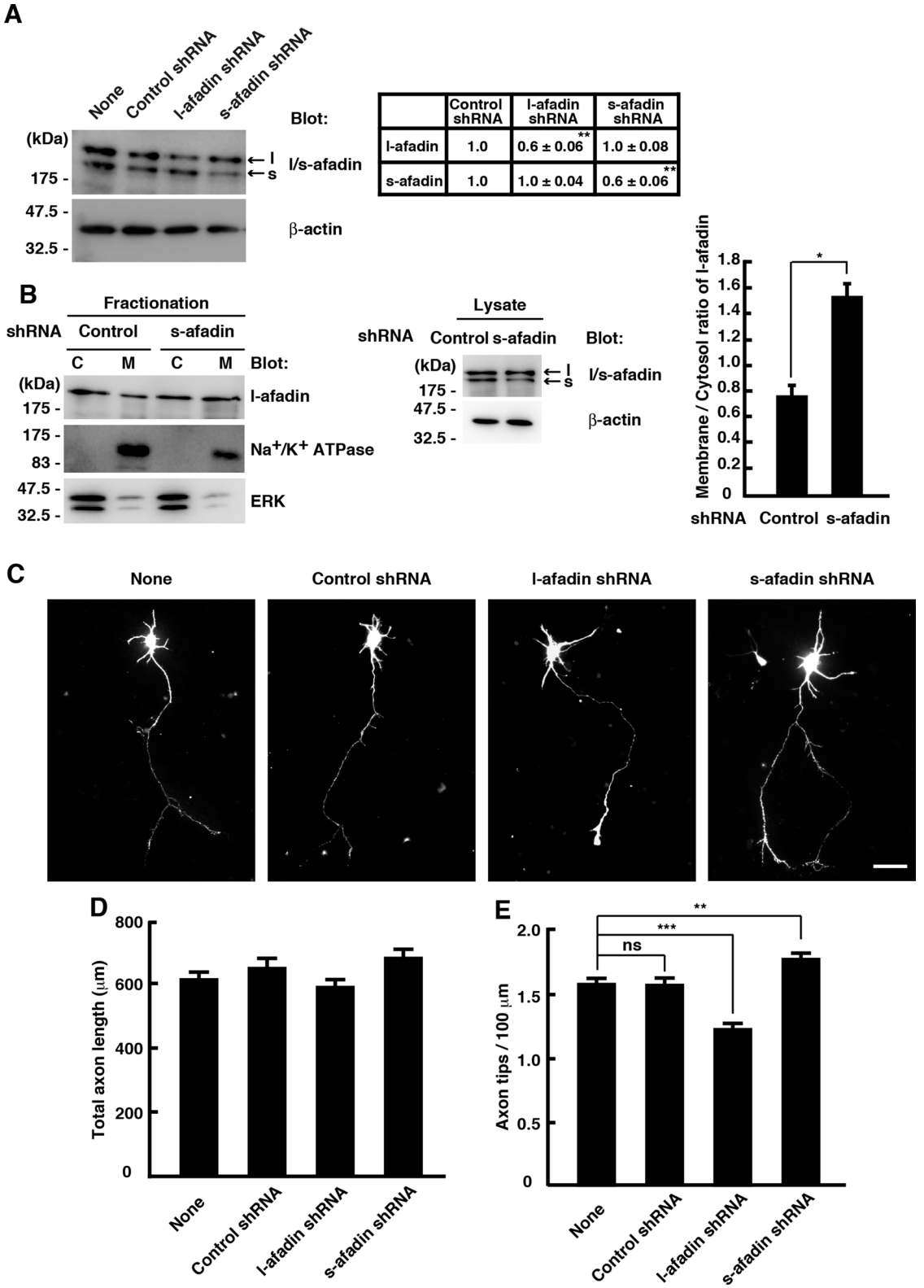

FIGURE 8: Knockdown of endogenous s-afadin promotes membrane translocation of l-afadin and axon branching. (A–C) Cortical neurons were transfected with the indicated plasmids at 0 DIV before plating using nucleofection technology. (A) Effect of l- or s-afadin–specific shRNA on endogenous l- and s-afadin proteins in 4-DIV neurons was verified by immunoblot analysis of whole-cell lysates with anti–l/s-afadin antibody. The immunoblots shown are representative of four independent experiments that yielded similar results. The table shows the quantification and statistical comparison of the expression level of the afadin isoforms in total cell lysate by densitometry of the immunoblots. The value of control shRNA-transfected cells was defined as 1, and relative fold expression was assessed ($n = 4$; means ± SEM; $^{**}p < 0.01$, one-way ANOVA with Dunnett's post hoc test). (B) Cellular homogenates from cultured

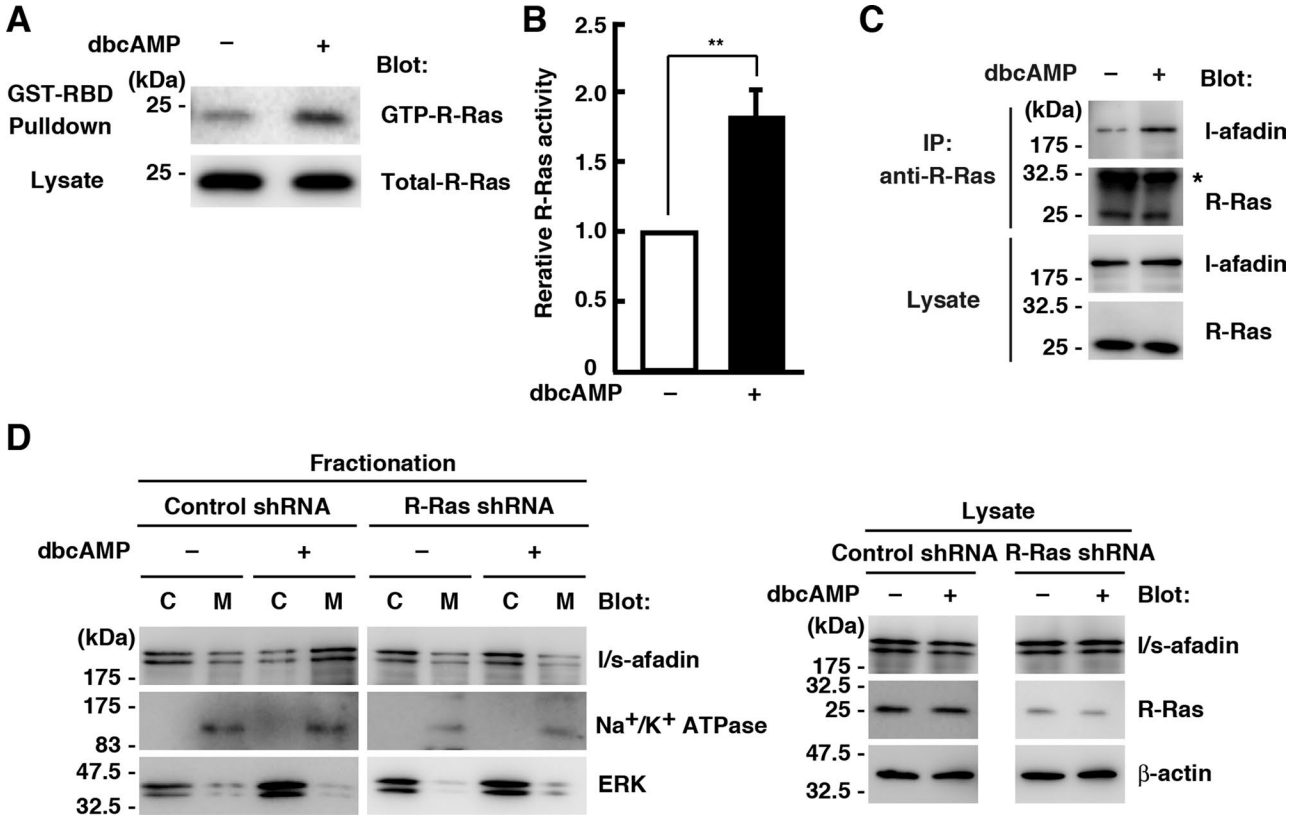

FIGURE 9: dbcAMP induces R-Ras activation and membrane localization of l-afadin. (A) Cortical neurons at 3 DIV were treated with dbcAMP (1 mM) or the corresponding vehicle control for 30 min. GTP-bound R-Ras isolated with GST-RBD was detected with an R-Ras antibody. (B) Relative R-Ras activity determined by the amount of R-Ras bound to GST-RBD normalized to the amount of R-Ras in cell lysates was analyzed by ImageJ software. The values are expressed as fold value of vehicle-treated cells, and the results are means ± SEM of three independent experiments (**$p < 0.01$; Student's *t* test) (C) Cell lysates from 3-DIV cortical neurons treated with dbcAMP (1 mM) or the corresponding vehicle control for 1 d were immunoprecipitated with anti-R-Ras antibody. Lysate inputs and immunoprecipitates were analyzed by immunoblotting. Asterisk indicates the position of the immunoglobulin light chains. (D) Cortical neurons were transfected with the indicated plasmids at 0 DIV before plating using nucleofection technology. Cellular homogenates from 3-DIV neurons treated with dbcAMP (1 mM) or the corresponding vehicle control for 1 d were separated into cytosolic (C) and membrane (M) fractions. The fractionated samples and total lysates were analyzed by immunoblotting. The results shown are representative of three independent experiments that yielded similar results.

subcellular localizations of s- and l-afadin proteins after cAMP treatment are totally the same. A recent study showed that s-afadin binds more preferentially to the cell adhesion molecules nectins than l-afadin, implying a specific role for s-afadin in cellular functions (Kobayashi *et al.*, 2014). It will be of interest to examine further whether s-afadin is colocalized with l-afadin in the specific F-actin–rich axonal membrane compartment, and membrane-localized s-afadin plays a distinct role in axonal development.

Isoform-specific knockdown of l-afadin suppresses axon branching but not axonal elongation, suggesting a specific role of l-afadin in axon branching rather than axonal outgrowth in cultured cortical neurons, and another mechanism contributes to axonal elongation. Intriguingly, however, expression of either R-Ras QL, a constitutively active form of R-Ras, or l-afadin-CAAX, a forced membrane targeting form of l-afadin, induces axon elongation as well as axon branching. It seems that global activation of R-Ras may induce nonspecific localization of endogenous l-afadin everywhere in the membrane of neurons, and l-afadin can potentially induce neurite elongation. Thus spatiotemporally regulated R-Ras activity within axon shafts may contribute to a specific role of

cortical neurons at 4 DIV were separated into cytosolic (C) and membrane (M) fractions. The fractionated samples and total lysates were analyzed by immunoblotting with anti–l-afadin antibody or anti–l/s-afadin antibody, respectively. The immunoblots shown are representative of three independent experiments that yielded similar results. The membrane/cytosol ratio of l-afadin was analyzed, and data are presented as the means ± SEM of three independent experiments (*$p < 0.05$, Student's *t* test). (A, B) Precise quantification graph data for knockdown efficiency are included in Supplemental Figure S2. (C) Neuronal morphology at 4 DIV was visualized by cotransfected YFP. Scale bar, 50 μm. (D, E) Total axon length (D) and axon tip number/100 μm (E) were measured. The results are means ± SEM of three independent experiments ($n = 45$; ns, not significant; **$p < 0.01$; ***$p < 0.001$, one-way ANOVA with Dunnett's post hoc test).

endogenous l-afadin in branching. Spatiotemporally regulated cAMP/protein kinase A signaling at the protrusive site along the axon shaft is supposed to be crucial for production of organized branching (Mingorance-Le Meur and O'Connor, 2009; Gallo, 2011). In nonneuronal cells, it has been reported that cAMP induces activation of R-Ras through activation of an R-Ras guanine nucleotide exchange factor, Epac (Mochizuki *et al.*, 2000; López De Jesús *et al.*, 2006). Consequently, we infer that locally elevated cAMP triggers local activation of Epac, thereby inducing local activation of R-Ras. Besides cAMP-mediated regulation of R-Ras activity, plexins—receptors for semaphorins—directly inactivate R-Ras in cultured neurons (Oinuma *et al.*, 2004a,b; Toyofuku *et al.*, 2005; Uesugi *et al.*, 2009). In addition, ephrins have also been reported to inactivate R-Ras activity to induce axonal repulsion (Dail *et al.*, 2006). Given the evidence that both attractive and repulsive guidance factors regulate R-Ras activity, R-Ras may serve as an integrator of multiple factors required for coordinated regulation of axon branching.

Corticospinal axons project collaterals into the pons, and the formation of the collateral branches are triggered by yet-unidentified factors secreted by pons, and branching occurs actively after the axons have passed the pons (Heffner *et al.*, 1990). Similar events have been reported for the branching of thalamocortical axons (Portera-Cailliau *et al.*, 2005). Further studies will be required to examine whether the R-Ras and l/s-afadin system contributes to spatiotemporal regulation of cortical axon branching in vivo.

MATERIALS AND METHODS

DNA constructs and mutagenesis

HA-tagged R-Ras QL (Q87L), a constitutively active mutant, R-Ras shRNA expression vectors, and the glutathione *S*-transferase (GST)–fused Ras-binding domain of c-Raf-1 (RBD; amino acids 53–130) have been described previously (Oinuma *et al.*, 2004a,b). GFP-tagged rat l-afadin (1–1829) was kindly provided by Y. Takai (Kobe University, Kobe, Japan). s-Afadin (1–1655) was obtained by reverse transcription-PCR from rat brain and deleted to produce s-afadin ΔRA (351–1655) by PCR-mediated mutagenesis. Myc-tagged l-afadin and s-afadin constructs were subcloned into pCXN2. pCAG vector encoding YFP was a generous gift from J. Miyazaki (Osaka University, Osaka, Japan) and T. Saito (Chiba University, Chiba, Japan). A CAAX sequence (where C represents cysteine, A is an aliphatic amino acid, and X is a terminal amino acid) was fused to the carboxyl terminal in-frame with l-afadin as described previously (Tasaka *et al.*, 2012). The shRNAs for two isoforms of afadin were designed to target 19 nucleotides of rat transcript and expressed by using pSinencer-2.1 (Invitrogen, Carlsbad, CA). The target sequences were as follows: l-afadin shRNA (nucleotides 5437–5455, 5′-GTGAAAGCTTCTCGTAAAT-3′); and s-afadin shRNA (3′ noncoding region, 5′-ATTAGCCTGAACACAAATG-3′). The shRNA for rat R-Ras (nucleotides 426–444, 5′-CAAGGCAGATCTGGAGACA-3′), which has no effect on R-Ras expression and axonal morphology (Oinuma *et al.*, 2007), was used as a control shRNA.

Antibodies and reagents

We used the following antibodies: mouse monoclonal antibodies against Myc (9E10), GFP (B-2) and l- and s-afadin (clone-35); rabbit polyclonal antibodies against HA (Y-11) (Santa Cruz Biotechnology, Santa Cruz, CA); a rabbit polyclonal anti-ERK antibody (Cell Signaling Technology, Beverly, MA); a rat monoclonal anti-HA antibody (3F10; Roche Applied Science, Indianapolis, IN); a mouse monoclonal anti-Na^+/K^+ ATPase α subunit antibody (Millipore, Billerica, MA); a mouse monoclonal anti–β-actin antibody (Sigma-Aldrich, St. Louis, MO); a rabbit polyclonal anti–l-afadin antibody (Abcam, Cambridge, MA); horseradish peroxidase (HRP)-conjugated secondary antibodies (DakoCytomation, Hamburg, Germany); and Alexa Fluor–conjugated secondary antibodies (Invitrogen). Rabbit anti–R-Ras antibody was generated against a keyhole limpet hemocyanin-conjugated synthetic peptide (RGRPRGGGPGPRDPPPGETHKC) corresponding to the amino terminus of mouse R-Ras. Poly-L-lysine and dbcAMP were from Sigma-Aldrich.

Cell culture and transfection

HEK293T cells and Neuro2a cells were cultured in DMEM containing 10% fetal bovine serum (FBS), 4 mM glutamine, 100 U/ml penicillin, and 0.2 mg/mL streptomycin under humidified air containing 5% CO_2 at 37°C. Transient transfections were carried out with Lipofectamine Plus (Invitrogen) for HEK293T cells or Lipofectamine 2000 (Invitrogen) for Neuro2a cells, according to the manufacturer's instructions.

Primary cortical neurons were prepared from the E19 rat brains as described previously (Iwasawa *et al.*, 2012). The dissociated neurons were seeded on poly-L-lysine–coated glass coverslips (circular, 13 mm in diameter) at a density of 2.5×10^4 cells or plastic dishes (60 mm or 100 mm in diameter) in DMEM containing 10% FBS, 4 mM glutamine, 100 U/ml penicillin, and 0.1 mg/ml streptomycin and cultured under humidified air containing 5% CO_2 at 37°C. After 4 h, the medium was replaced with Neurobasal medium (Invitrogen) containing 2% B27 supplement (Invitrogen), 0.5 mM GlutaMAX (Invitrogen), 50 U/ml penicillin, and 0.05 mg/ml streptomycin, and neurons were cultured under humidified air containing 5% CO_2 at 37°C. For overexpression experiments, cortical neurons were transfected with the indicated plasmids at 1 DIV with Lipofectamine 2000 according to the manufacturer's instructions. For knockdown and R-Ras QL and s-afadin expression, transfection was performed by Rat Neuron Nucleofector kit (Lonza, Basel, Switzerland) following the manufacturer's instructions (program O-003). dbcAMP was dissolved in water, and pharmacological treatment (dbcAMP 1 mM or water vehicle) was performed for 30 min (for analysis on R-Ras activity) or 1 d (for subcellular localization and morphological analyses) before fixation. All animal experiments were conducted according to the guidelines of the Kyoto University Research Committee.

Preparation of rat brain homogenates

Brains of Wistar rats were homogenized with a Teflon homogenizer in homogenizing buffer (20 mM Tris-HCl, pH 7.4, 0.32 M sucrose, 10 mM $MgCl_2$, 1 mM EDTA, 1 μg/ml aprotinin, 1 μg/ml leupeptin, 0.1 mM benzamidine, 0.2 mM phenylmethylsulfonyl fluoride [PMSF]). The homogenates (containing 50 μg of total protein) were lysed with Laemmli sample buffer and analyzed by immunoblotting.

Immunoblotting

Proteins were separated by SDS–PAGE and electrophoretically transferred onto a polyvinylidene difluoride membrane (Millipore). The membrane was blocked with 3% low-fat milk in Tris-buffered saline (TBS) and then incubated with primary antibodies. The primary antibodies were detected with HRP-conjugated secondary antibodies and a chemiluminescence detection Kit (ECL; GE Healthcare, Piscataway, NJ). Images were captured using a LAS3000 analyzer (Fuji, Tokyo, Japan) equipped with Science Lab software (Fuji).

Measurement of R-Ras activity

Measurement of R-Ras activity in neurons was performed as described previously (Oinuma *et al.*, 2007). Cortical neurons (2.5×10^6 cells)

at 3 DIV treated with 1 mM dbcAMP for 30 min were lysed directly on dishes with ice-cold cell lysis buffer (25 mM 4-(2-hydroxyethyl)-1-piperazineethanesulfonic acid–NaOH, pH 7.5, 150 mM NaCl, 10 mM $MgCl_2$, 0.5% Nonidet P-40, 0.5% sodium deoxycholate, 1 mM EDTA, 25 mM NaF, 1 mM orthovanadate, 1 mM PMSF, 10 µg/ml aprotinin, 10 µg/ml leupeptin, and 1 mM dithiothreitol) containing 75 µg GST-RBD of cRaf-1.

Immunoprecipitation

Immunoprecipitation was performed as described previously (Iwasawa *et al.*, 2012). HEK293T cells transfected with indicated plasmids were washed with TBS and lysed with the ice-cold IP buffer (20 mM Tris-HCl, pH 8.0, 150 mM NaCl, 4 mM $MgCl_2$, 1% NP-40, 10% glycerol, 1 mM PMSF, 10 µg/ml aprotinin, 10 µg/ml leupeptin). The cell lysates were then centrifuged for 5 min at 16,000 × *g* at 4°C. The cleared supernatants were incubated with anti-HA antibody (Y-11) for 2 h and subsequently with protein G–Sepharose (GE Healthcare) for 1 h. The beads were washed with ice-cold IP buffer, and bound proteins were analyzed by SDS–PAGE and immunoblotting. For the detection of endogenous protein binding, primary cultured cortical neurons treated with 1 mM dbcAMP for 1 d were lysed at 3 DIV with ice-cold IP buffer. After centrifugation for 10 min at 16,000 × *g* at 4°C, the supernatants were incubated with anti–R-Ras 1 µg of antibody for 1 h and then with protein G-Sepharose beads for 1 h. The beads were washed with ice-cold IP buffer, and bound proteins were analyzed by SDS–PAGE and immunoblotting.

Separation of membrane and cytosol fractions

Separation of membrane and cytosol fractions was performed as described previously (Iwasawa *et al.*, 2012). Briefly, Neuro2a cells transfected with indicated plasmids were washed with TBS and suspended in ice-cold buffer A (20 mM Tris-HCl, pH 7.5, 150 mM NaCl, 50 mM NaF, 1 mM Na_3VO_4, and 1 mM PMSF). After rapid freezing in liquid nitrogen and thawing in a water bath, cells were centrifuged for 10 min at 16,000 × *g* at 4°C. The supernatants were removed and used as cytosol fractions. The pellets were washed with buffer A and lysed with buffer A containing 1% Triton X-100. After centrifugation for 10 min at 10,000 × *g* at 4°C, the supernatants were used as membrane fractions. Both cytosol and membrane fractions were analyzed by SDS–PAGE and immunoblotting.

Immunofluorescence microscopy

Immunofluorescence microscopy was performed as described previously (Iwasawa *et al.*, 2012). Neuro2a cells and primary cultured neurons on coverslips were fixed with 4% paraformaldehyde in phosphate-buffered saline (PBS) for 20 min. After residual paraformaldehyde had been quenched with 50 mM NH_4Cl in PBS for 10 min, cells were permeabilized with 0.2% Triton X-100 in PBS for 10 min and incubated with 10% FBS in PBS for 30 min. Cells were incubated with the primary antibodies for 1 h, followed by incubation with Alexa 594–conjugated secondary antibodies for 1 h. The cells on coverslips were mounted in 90% glycerol containing 0.1% *p*-phenylenediamine dihydrochloride in PBS and photographed with a Leica DC350F digital camera system (Leica, Wetzlar, Germany) equipped with a Nikon Eclipse E800 microscope (Nikon, Tokyo, Japan). The images were arranged and labeled using Photoshop CS5.1 (Adobe, San Jose, CA).

Data analysis

Protein densitometry analysis was performed using ImageJ software (National Institutes of Health, Bethesda, MD). Quantification of axonal morphology was performed as described previously (Iwasawa *et al.*, 2012). A process that was at least twice as long as the other processes and was more than twice the cell body diameter was defined as an axon, as described elsewhere (Schwamborn and Püschel 2004; Sepúlveda *et al.*, 2009), and total length and tip number were measured. The processes >5 µm in length were counted and defined as "tip number" (Marler *et al.*, 2008). The length of each neurite was measured from the edge of the cell body (or its branching point) to the tip of the neurite, and total axon length means the sum of the lengths of all of the axons of the neuron. Statistical significance was determined by the analysis of variance (ANOVA) and post hoc test (Dunnett T3) or Student's *t* test using SPSS software (version 16.0; SPSS). Differences at the level of $p < 0.05$ were considered statistically significant. The immunoblot data shown are the representative of three independent experiments that yielded similar results.

ACKNOWLEDGMENTS

We thank Y. Takai, J. Miyazaki, and T. Saito for providing expression plasmids. This research was supported by the Japan Science and Technology Agency PRESTO Project (Development and Function of Neuronal Networks), Grants-in-Aid for Scientific Research from the Ministry of Education, Culture, Sports, Science and Technology of Japan (Scientific Research on Innovative Areas 25123708 and Challenging Exploratory Research 26640043), grants from the Mitsubishi Foundation, and an Inoue Science Research Award (all to I.O.).

REFERENCES

Boldface names denote co–first authors.

Arimura N, Kaibuchi K (2007). Neuronal polarity: from extracellular signals to intracellular mechanisms. Nat Rev Neurosci 8, 194–205.

Asada M, Irie K, Morimoto K, Yamada A, Ikeda W, Takeuchi M, Takai Y (2003). ADIP, a novel afadin- and alpha-actinin-binding protein localized at cell-cell adherens junctions. J Biol Chem 278, 4103–4111.

Bradke F, Dotti CG (2000). Establishment of neuronal polarity: lessons from cultured hippocampal neurons. Curr Opin Neurobiol 10, 574–581.

Beaudoin GM 3rd, Schofield CM, Nuwal T, Zang K, Ullian EM, Huang B, Reichardt LF (2012). Afadin, a ras/rap effector that controls cadherin function, promotes spine and excitatory synapse density in the hippocampus. J Neurosci 32, 99–110.

Bilimoria PM, Bonni A (2013). Molecular control of axon branching. Neuroscientist 19, 16–24.

Corset V, Nguyen-Ba-Charvet KT, Forcet C, Moyse E, Chédotal A, Mehlen P (2000). Netrin-1-mediated axon outgrowth and cAMP production requires interaction with adenosine A2b receptor. Nature 407, 747–750.

Dail M, Richter M, Godement P, Pasquale EB (2006). Eph receptors inactivate R-Ras through different mechanisms to achieve cell repulsion. J Cell Sci 119, 1244–1254.

Dent EW, Kalil K (2001). Axon branching requires interactions between dynamic microtubules and actin filaments. J Neurosci 21, 9757–9769.

Dent EW, Barnes AM, Tang F, Kalil K (2004). Netrin-1 and semaphorin 3A promote or inhibit cortical axon branching, respectively, by reorganization of the cytoskeleton. J Neurosci 24, 3002–3012.

Fournier G *et al.* (2011). Loss of AF6/afadin, a marker of poor outcome in breast cancer, induces cell migration, invasiveness and tumor growth. Oncogene 30, 3862–3874.

Gallo G (2011). The cytoskeletal and signaling mechanisms of axon collateral branching. Dev Neurobiol 71, 201–220.

Grabowski PJ, Black DL (2001). Alternative RNA splicing in the nervous system. Prog Neurobiol 65, 289–308.

Hall A, Lalli G (2010). Rho and Ras GTPases in axon growth, guidance, and branching. Cold Spring Harb Perspect Biol 2, a001818.

Heffner CD, Lumsden AD, O'Leary DD (1990). Target control of collateral extension and directional growth in the mammalian brain. Science 247, 217–220.

Höpker VH, Shewan D, Tessier-Lavigne M, Poo M, Holt C (1999). Growth cone attraction is converted to repulsion by laminin. Nature 401, 69–73.

Ito Y, Oinuma I, Katoh H, Kaibuchi K, Negishi M (2006). Sema4D/plexin-B1 activates GSK-3β through R-Ras GAP activity, inducing growth cone collapse. EMBO Rep 7, 704–709.
Iwasawa N, Negishi M, Oinuma I (2012). R-Ras controls axon branching through afadin in cortical neurons. Mol Biol Cell 23, 2793–2804.
Kalil K, Szebenyi G, Dent EW (2000). Common mechanisms underlying growth cone guidance and axon branching. J Neurobiol 44, 145–158.
Keely PJ, Rusyn EV, Cox AD, Parise LV (1999). R-Ras signals through specific integrin alpha cytoplasmic domains to promote migration and invasion of breast epithelial cells. J Cell Biol 145, 1077–1088.
Kinbara K, Goldfinger LE, Hansen M, Chou FL, Ginsberg MH (2003). Ras GTPases: integrin's friends or foes? Nat Rev Mol Cell Biol 4, 767–776.
Kobayashi R, Kurita S, Miyata M, Maruo T, Mandai K, Rikitake Y, Takai Y (2014). s-Afadin binds more preferentially to the cell adhesion molecules nectins than l-afadin. Genes Cells 19, 853–863.
Komatsu M, Ruoslahti E (2005). R-Ras is a global regulator of vascular regeneration that suppresses intimal hyperplasia and tumor angiogenesis. Nat Med 11, 1346–1350.
Kurita S, Ogita H, Takai Y (2011). Cooperative role of nectin-nectin and nectin-afadin interactions in formation of nectin-based cell-cell adhesion. J Biol Chem 286, 36297–36303.
Liedtke M, Ayton PM, Somervaille TC, Simith KS, Cleary ML (2010). Self-association mediated by the Ras association 1 domain of AF6 activates the oncogenic potential of MLL-AF6. Blood 116, 63–70.
Lim ST, Lim KC, Giuliano RE, Federoff HJ (2008). Temporal and spatial localization of nectin-1 and l-afadin during synaptogenesis in hippocampal neurons. J Comp Neurol 507, 1228–1244.
López De Jesús ML, Stope MB, Oude Weernink PA, Mahlke Y, Börgermann C, Ananaba VN, Rimmbach C, Rosskopf D, Michel MC, Jakobs KH, Schmidt M (2006). Cyclic AMP-dependent and Epac-mediated activation of R-Ras by G-protein-coupled receptors leads to phospholipase D stimulation. J Biol Chem 281, 21837–21847.
Loudon RP, Silver LD, Yee HF Jr, Gallo G (2006). RhoA-kinase and myosin II are required for the maintenance of growth cone polarity and guidance by nerve growth factor. J Neurobiol 66, 847–867.
Mandai K, Nakanishi H, Satoh A, Obaishi H, Wada M, Nishioka H, Ito M, Mizoguchi A, Aoki T, Fujimoto T, *et al.* (1997). Afadin: A novel actin filament-binding protein with one PDZ domain localized at cadherin-based cell-to-cell adherens junction. J Cell Biol 139, 517–528.
Marler KJ, Becker-Barroso E, Martínez A, Llovera M, Wentzel C, Poopalasundaram S, Hindges R, Soriano E, Comella J, Drescher U (2008). A TrkB/EphrinA interaction controls retinal axon branching and synaptogenesis. J Neurosci 28, 12700–12712.
Matsumoto K, Asano T, Endo T (1997). Novel small GTPase M-Ras participates in reorganization of actin cytoskeleton. Oncogene 15, 2409–2417.
Mingorance-Le Meur A, O'Connor TP (2009). Neurite consolidation is an active process requiring constant repression of protrusive activity. EMBO J 28, 248–260.
Miyata M, Ogita H, Komura H, Nakata S, Okamoto R, Ozaki M, Majima T, Matsuzawa N, Kawano S, Minami A, *et al.* (2009). Localization of nectin-free afadin at the leading edge and its involvement in directional cell movement induced by platelet-derived growth factor. J Cell Sci 122, 4319–4329.
Mochizuki N, Ohba Y, Kobayashi S, Otsuka N, Graybiel AM, Tanaka S, Matsuda M (2000). Crk activation of JNK via C3G and R-Ras. J Biol Chem 275, 12667–12671.
O'Donnell M, Chance RK, Bashaw GJ (2009). Axon growth and guidance: receptor regulation and signal transduction. Annu Rev Neurosci 32, 383–412.
Oinuma I, Ishikawa Y, Katoh H, Negishi M (2004a). The Semaphorin 4D receptor Plexin-B1 is a GTPase activating protein for R-Ras. Science 305, 862–865.
Oinuma I, Katoh H, Negishi M (2004b). Molecular dissection of the semaphorin 4D receptor plexin-B1-stimulated R-Ras GTPase-activating protein activity and neurite remodeling in hippocampal neurons. J Neurosci 24, 11473–11480.
Oinuma I, Katoh H, Negishi M (2007). R-Ras controls axon specification upstream of glycogen synthase kinase-3beta through integrin-linked kinase. J Biol Chem 282, 303–318.
Pokutta S, Drees F, Takai Y, Nelson WJ, Weis WI (2002). Biochemical and structural definition of the l-afadin- and actin-binding sites of alpha-catenin. J Biol Chem 277, 18868–18874.
Portera-Cailliau C, Weimer RM, De Paola V, Caroni P, Svoboda K (2005). Diverse modes of axon elaboration in the developing neocortex. PLoS Biol 3, e272.
Schreiner D, Nguyen TM, Russo G, Heber S, Patrignani A, Ahmé E, Scheiffele P (2014). Targeted combinatorial alternative splicing generates brain region-specific repertoires of neurexins. Neuron 84, 386–398.
Schwamborn JC, Püschel AW (2004). The sequential activity of the GTPases Rap1B and Cdc42 determines neuronal polarity. Nat Neurosci 7, 923–929.
Sepúlveda MR, Vanoevelen J, Raeymaekers L, Mata AM, Wuytack F (2009). Silencing the SPCA1 (secretory pathway $Ca2^{+}$-ATPase isoform 1) impairs $Ca2^{+}$ homeostasis in the Golgi and disturbs neural polarity. J Neurosci *29*, 12174–12182.
Spillane M, Gallo G (2014). Involvement of Rho-family GTPases in axon branching. Small GTPases 5, e27974.
Tachibana K, Nakanishi H, Mandai K, Ozaki K, Ikeda W, Yamamoto Y, Nagafuchi A, Tsukita S, Takai Y (2000). Two cell adhesion molecules, nectin and cadherin, interact through their cytoplasmic domain-associated proteins. J Cell Biol 150, 1161–1176.
Takahashi K, Nakanishi H, Miyahara M, Mandai K, Satoh K, Satoh A, Nishioka H, Aoki J, Nomoto A, Mizoguchi A, *et al.* (1999). Nectin/PRR: an immunoglobulin-like cell adhesion molecule recruited to cadherin-based adherens junctions through interaction with Afadin, a PDZ domain-containing protein. J Cell Biol 145, 539–549.
Takai Y, Ikeda W, Ogita H, Rikitake Y (2008). The immunoglobulin-like cell adhesion molecule nectin and its associated protein afadin. Annu Rev Cell Dev Biol 24, 309–342.
Tasaka G, Negishi M, Oinuma I (2012). Semaphorin 4D/Plexin-B1-mediated M-Ras GAP activity regulates actin-based dendrite remodeling though Lamellipodin. J Neurosci 32, 8293–8305.
Tojima T, Hines JH, Henley JR, Kamiguchi H (2011). Second messengers and membrane trafficking direct and organize growth cone steering. Nat Rev Neurosci 12, 191–203.
Toyofuku T, Yoshida J, Sugimoto T, Zhang H, Kumanogoh A, Hori M, Kikutani H (2005). FARP2 triggers signals for Sema3A-mediated axonal repulsion. Nat Neurosci 8, 1712–1719.
Uesugi K, Oinuma I, Katoh H, Negishi M (2009). Different requirement for Rnd GTPases of R-Ras GAP activity of Plexin-C1 and Plexin-D1. J Biol Chem 284, 6743–6751.
Xie Z, Huganir RL, Penzes P (2005). Activity-dependent dendritic spine structural plasticity is regulated by small GTPase Rap1 and its target AF-6. Neuron 48, 605–618.
Yamada A, Uesaka N, Hayano Y, Tabata T, Kano M, Yamamoto N (2010). Role of pre- and postsynaptic activity in thalamocortical axon branching. Proc Natl Acad Sci USA 107, 7562–7567.
Zhang Z, Vuori K, Wang H, Reed JC, Ruoslahti E (1996). Integrin activation by R-ras. Cell 85, 61–69.